Spatially resolved modelling of immune responses following a multiscale approach

Dmitry Grebennikov,[1,2] Gennady Bocharov[1]

[1]Marchuk Institute of Numerical Mathematics, Russian Acedemy of Sciences
[2]Peoples' Friendship University of Russia (RUDN University)

The 11th Workshop on Biomath
The Week of Applied Mathematics and Mathematical Modelling
FEFU, Vladivostok
10.10.2019

Scales of human immune system organization

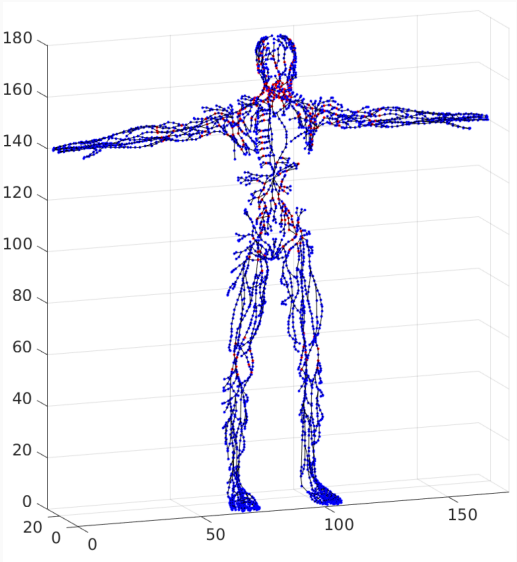

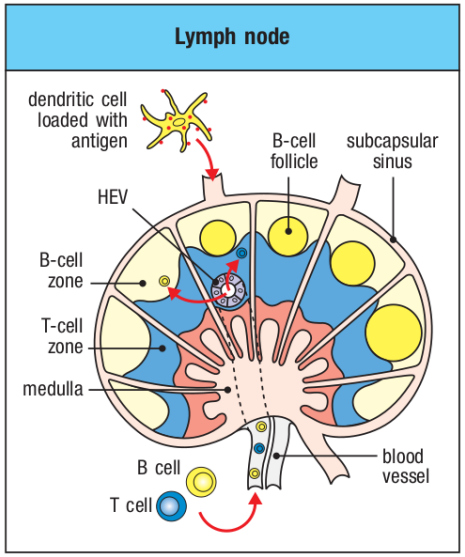

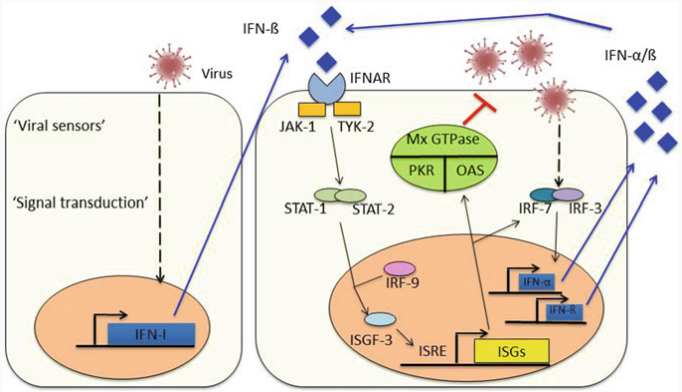

Tretyakova et al. Developing Comp Geometry and Network Graph Models of Human Lymphatic System, 2017

Janeway's Immunobiology, 9th edition, 2017

Bocharov et al. Mathematical Immunology of Virus Infections, 2018

Scales of human immune system organization

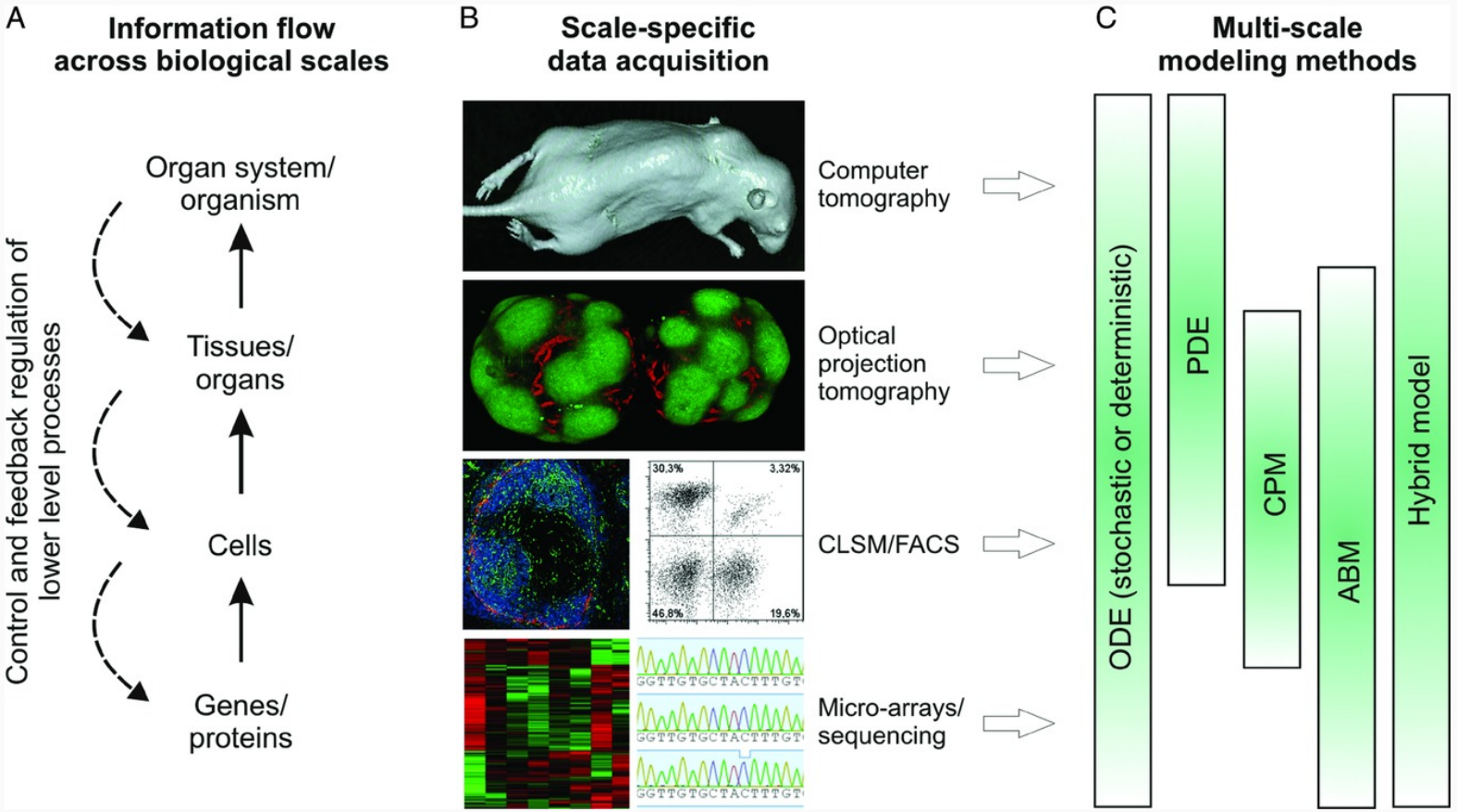

Ludewig et al. A global ”imaging” view on systems approaches in immunology, 2012

Lymph node structure

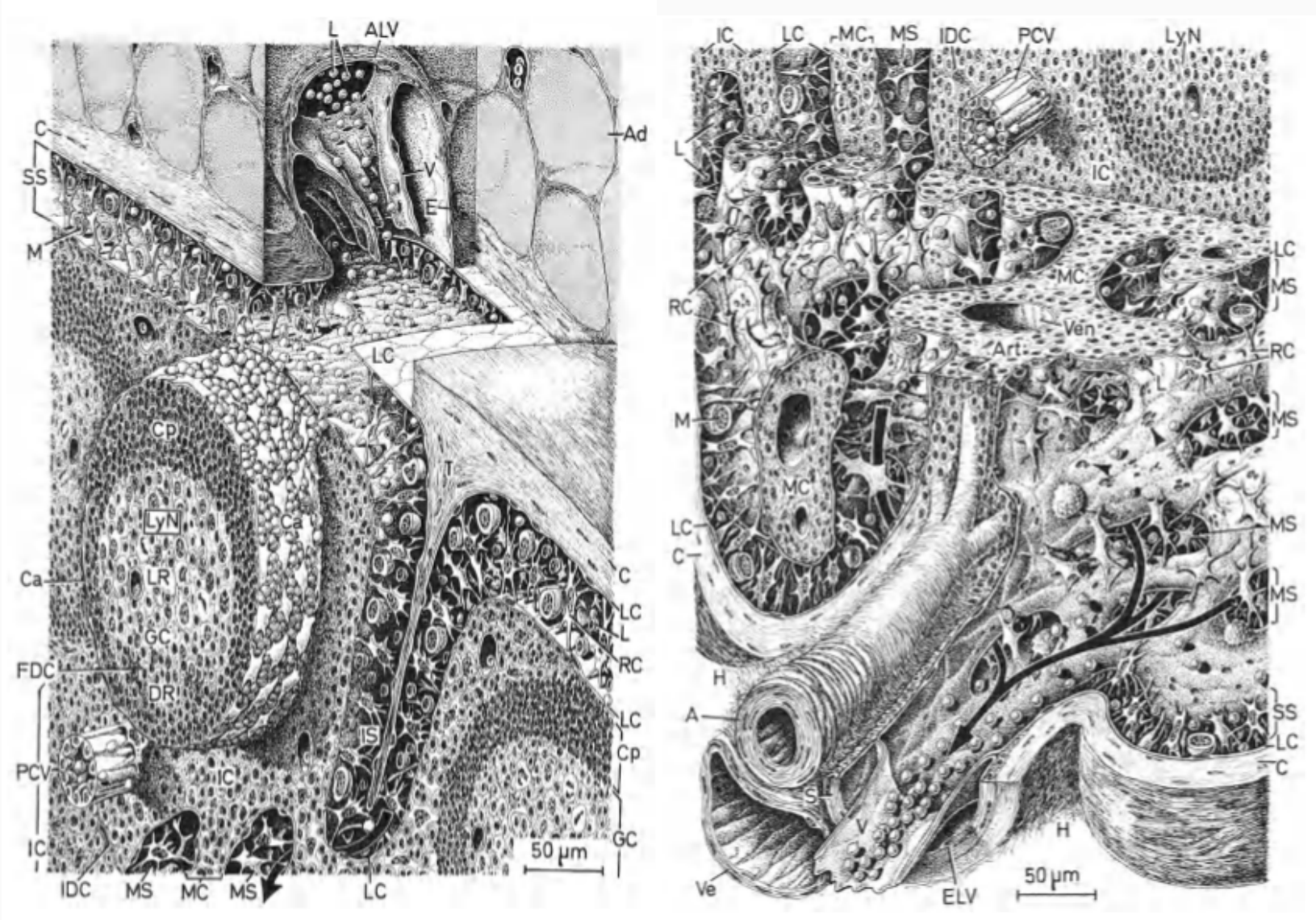

Krstic, Human Microscopic Atlas, 1994

Lymph node structure

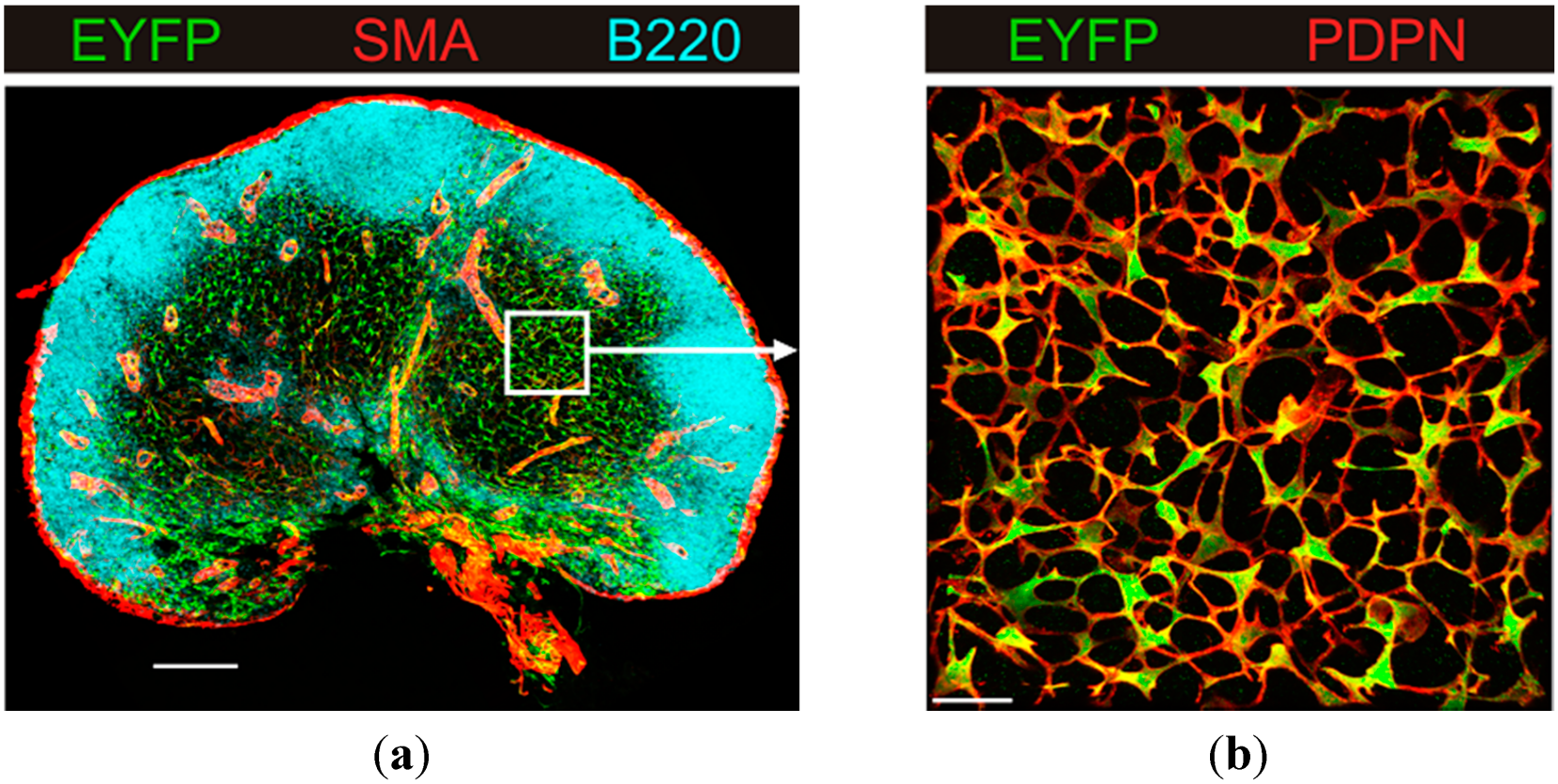

Kislitsyn et al. Computational approach to 3D modeling of the lymph node geometry. 2015

Hybrid multiscale modelling

Hybrid 2D model of HIV infection in lymph node

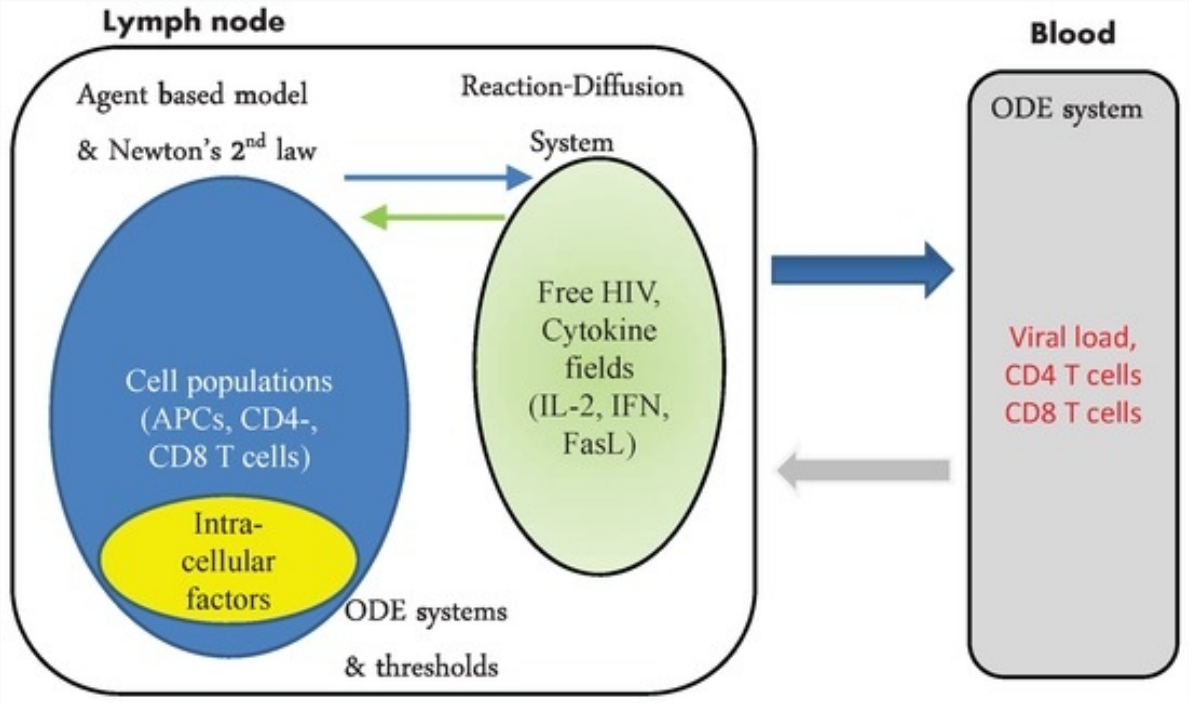

Bouchnita A, Bocharov G, Meyerhans A, Volpert V. Towards a Multiscale Model of Acute HIV Infection. Computation 2017; 5:6.

Hybrid 2D model of HIV infection in lymph node

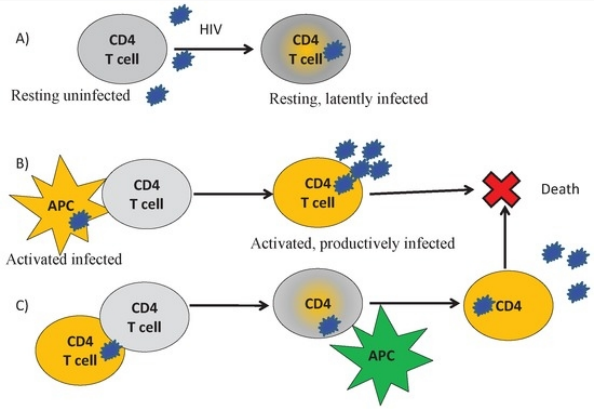

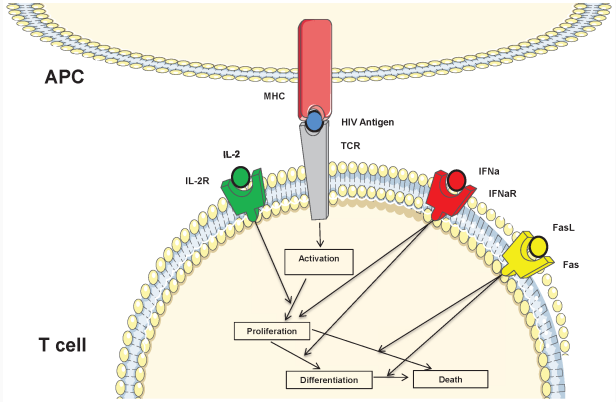

- Bouchnita A, Bocharov G, Meyerhans A, Volpert V. Towards a Multiscale Model of Acute HIV Infection. Computation 2017; 5:6.
- Bouchnita A, Bocharov G, Meyerhans A, Volpert V. Hybrid approach to model the spatial regulation of T cell responses. BMC Immunology 2017; 18:29.

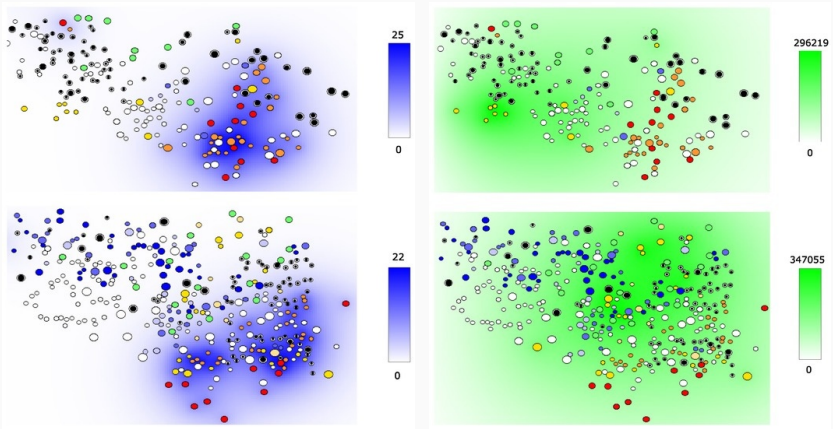

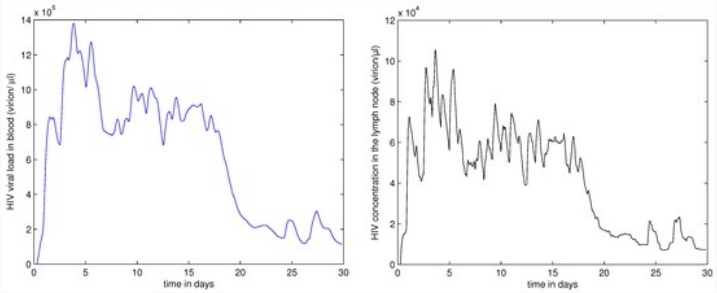

Modelling immune cell motility

Experimental data of lymphocyte motility

Trajectories of T cell migration
(*in vivo* microscopy of T cell zone of murine lymph nodes):

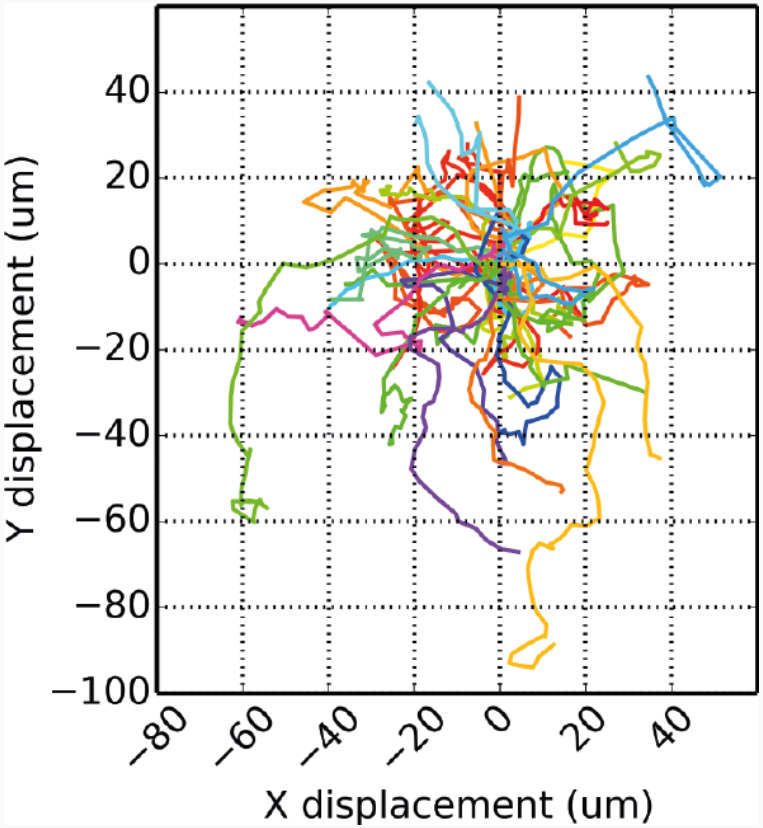

Read et al. Leukocyte Motility Models Assessed through Simulation and Multi-objective Optimization-Based Model Selection. 2016

Metrics characterizing the motility of immune cells

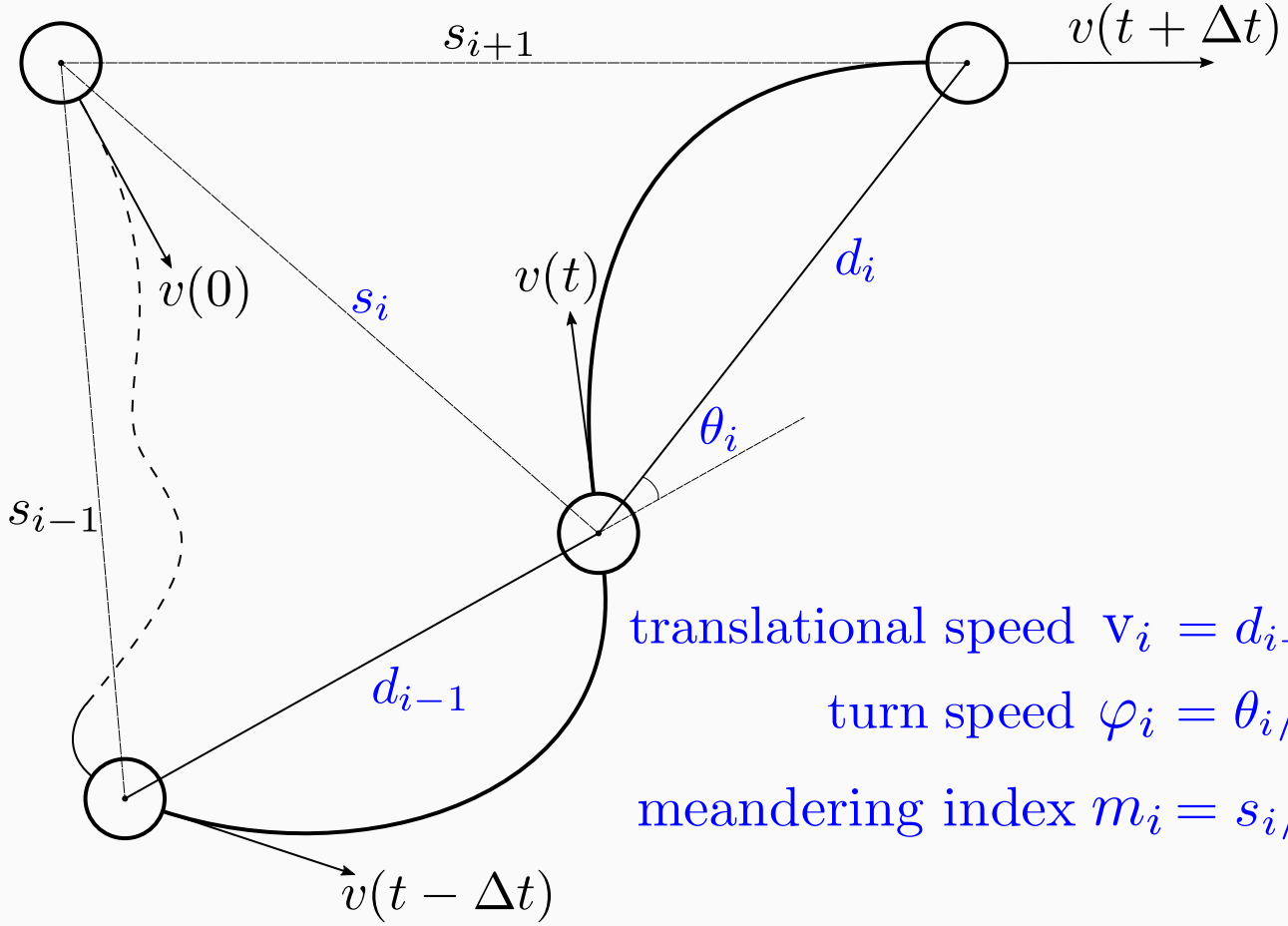

$$\text{translational speed } \mathrm{v}_i = d_{i-1}/\Delta t$$

$$\text{turn speed } \varphi_i = \theta_i/\Delta t$$

$$\text{meandering index } m_i = s_i / \sum_{k=0}^{i-1} d_k$$

Empirical distributions (statistical profile)

E

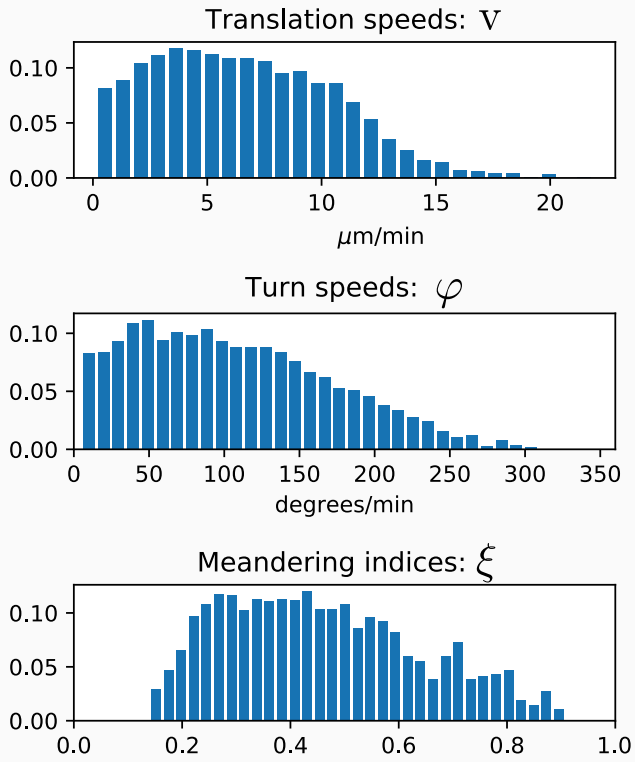

Read et al. Leukocyte Motility Models Assessed through Simulation and Multi-objective Optimization-Based Model Selection. 2016

Existing types of cell motility models

- Agent-based models
- Based on classical mechanics equations (isotropic particle models, dissipative particle dynamics)
- Based on energetic formulation of cell systems (cellular Potts model, phase-field models)

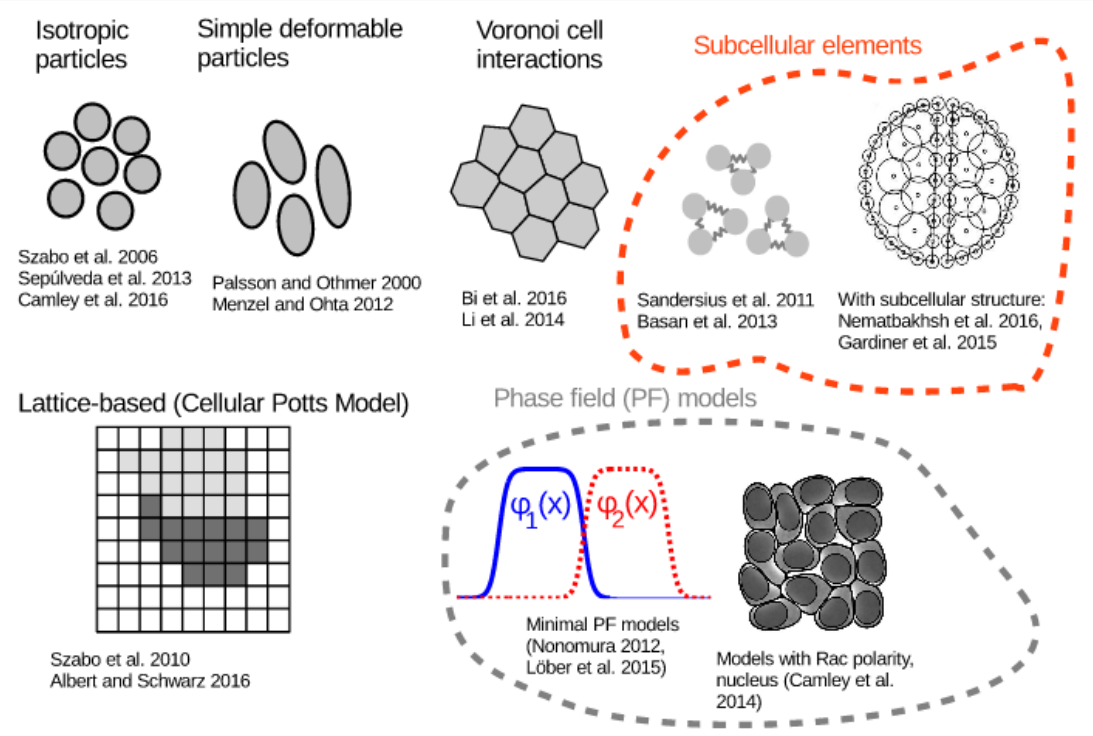

Camley, Rappel. Physical models of collective cell motility: from cell to tissue. 2017

Model of cell motility (isotropic particle model)

Equations governing the cell movement

$$m_i \ddot{\mathbf{x}}_i = \mathbf{F}_i = \sum_{j \neq i} \mathbf{f}_{ij} + \mathbf{f}_i^r - \mu \dot{\mathbf{x}}_i \quad \text{in} \quad \Omega$$

include

- dissipative friction forces $-\mu \dot{\mathbf{x}}_i$,
- cell-to-cell interaction forces $\sum_{j \neq i} \mathbf{f}_{ij}$,
- stochastic force of active (intrinsic) cell motility $\mathbf{f}_i^r$.

Cell-to-cell interaction forces f_{ij}

C

$$a, b : \mathbf{f_{ij}^{int}}(\lambda r_j) = \mathbf{f_{ij}^{int}}(r_j) = 0, \min_x \mathbf{f_{ij}^{int}}(x) = -f_i^{adh}$$

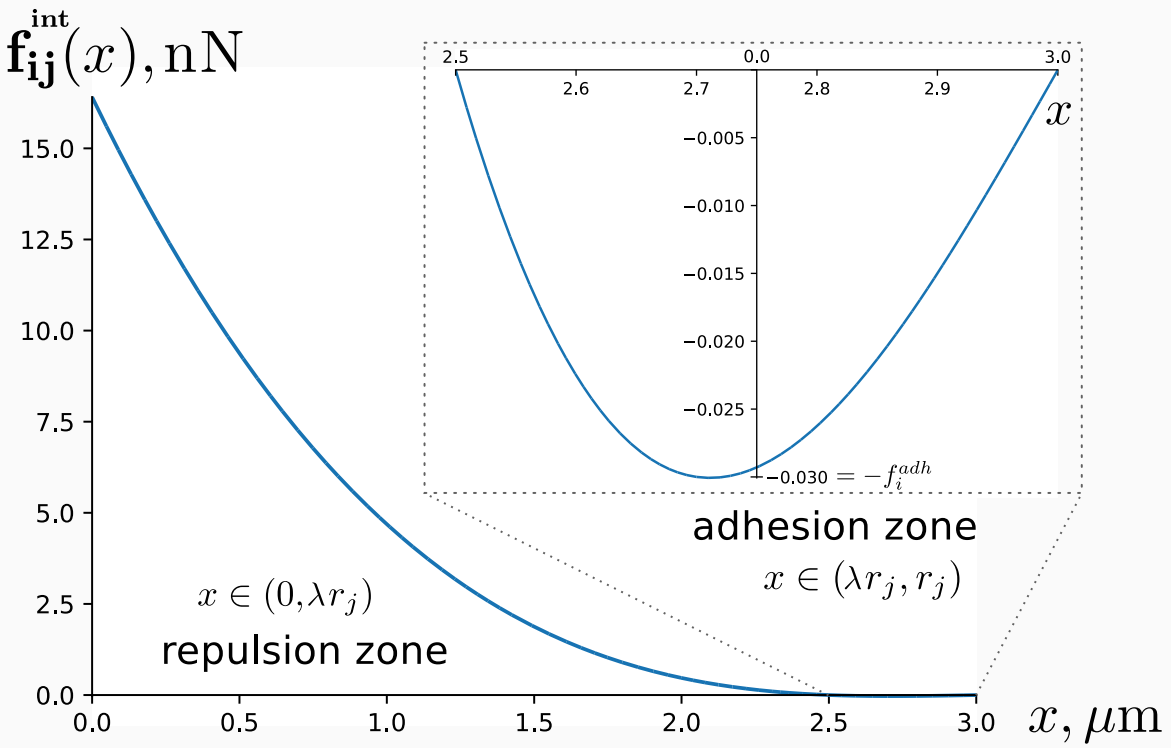

$$\mathbf{f_{ij}^{int}} = \frac{\mathbf{x_i} - \mathbf{x_j}}{h_{ij}} \cdot \begin{cases} -a \cdot f_i^{adh} \frac{r_j - x}{r_j} + b \cdot f_i^{adh} \frac{(r_j - x)^3}{r_j^3}, & h_{ij} < r_i + r_j, \\ 0, & h_{ij} \geqslant r_i + r_j \end{cases}$$

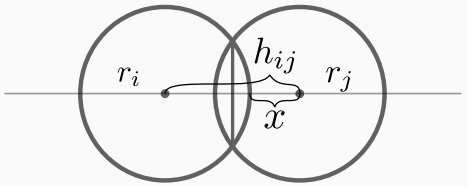

Cell-to-cell interaction forces f_{ij}

Force of cell-cell adhesion (minimum of $\mathbf{f}_{ij}(x)$) is estimated by the data on single-cell force spectroscopy*:

$$\mathbf{f}^{adh}_{TC-TC} \approx 0.01nN$$

$$\mathbf{f}^{adh}_{TC-DC} \approx 1nN$$

*Lim et al. CD80 and CD86 Differentially Regulate Mechanical Interactions of T-Cells with Antigen-Presenting Dendritic Cells and B-Cells. 2012

The force of active motility f_i^r

The force of active motility *implicitly* describes the guidance of T cells by stromal structure using empirical model of correlated random walk.

- Sampling is based on empirical model for velocities IHomoCRW[1], which fits well the empirical statistical profile.
- The force sampled by rules of IHomoCRW is corrected based on model of contact inhibition of locomotion[2] (CIL).

[1] Read et al. Leukocyte Motility Models Assessed through Simulation and Multi-objective Optimization-Based Model Selection. 2016

[2] Zimmermann et al. Contact inhibition of locomotion determines cell-cell and cell-substrate forces in tissues. 2016

The force of active motility (m_i, without CIL)

Every $\Delta t = 30$ seconds the magnitude and direction of force are updated. The force magnitude is sampled from normal distribution:

$$K_i^r \in |N(\mu(K^r), \sigma(K^r))|$$

The angle θ, by which the direction of force is changed, is determined by equations:

$$\alpha \in N(0, \sigma(\alpha)), \quad \theta = \alpha \cdot \left(1 - \left(\frac{K_i^r}{K_{max}^r}\right)^{\beta}\right),$$

where β — scalar coefficient, which parametrizes the inverse relation between translational speed and turning angle speed.

We estimated $\mu(K^r) = 3$ nN, $K_{max}^r = 3.9$ nN
(compare with $\sim$5 nN forces exerted by a CTL to destruct the membrane of a target cell).

The force of active motility ($\mathbf{f}_i^r$, correction by CIL)

$$\mathbf{f}_i^* = c_{inh}\hat{\mathbf{m}}_i + \hat{\mathbf{R}}_i,$$

$$\hat{\mathbf{R}}_i = \sum_{j, h_{ij} \leqslant r_i + r_j} \frac{\mathbf{x}_i - \mathbf{x}_j}{h_{ij}},$$

$$\mathbf{f}_i^r = -\frac{K_i^r \mathbf{f}_i^*}{c_{inh} + n},$$

where K_i^r — the magnitude of motility force (without CIL-correction),
n — number of contacting neighboring cells,
$\hat{\mathbf{m}}_i$ — the direction of motility force,
$\hat{\mathbf{R}}_i$ determines the shift of force direction due to CIL,
c_{inh} — weighting coefficient determining CIL level.

Model calibration

Model calibration by experimental data

Protocol to obtain statistical profile:

F

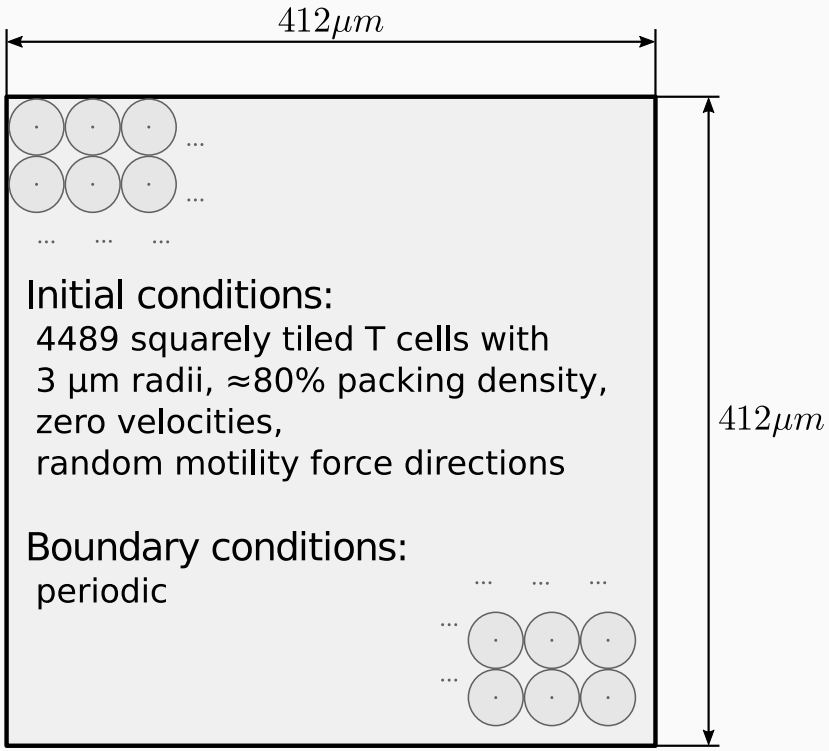

Protocol:
* 30-min pre-run to randomly mix cells
* 10 experiments of 30 minutes length
* save cell positions every 30 seconds
* exclude cells with total displacement < 27 μm
* exclude cells passed through periodic boundaries

Model calibration by experimental data

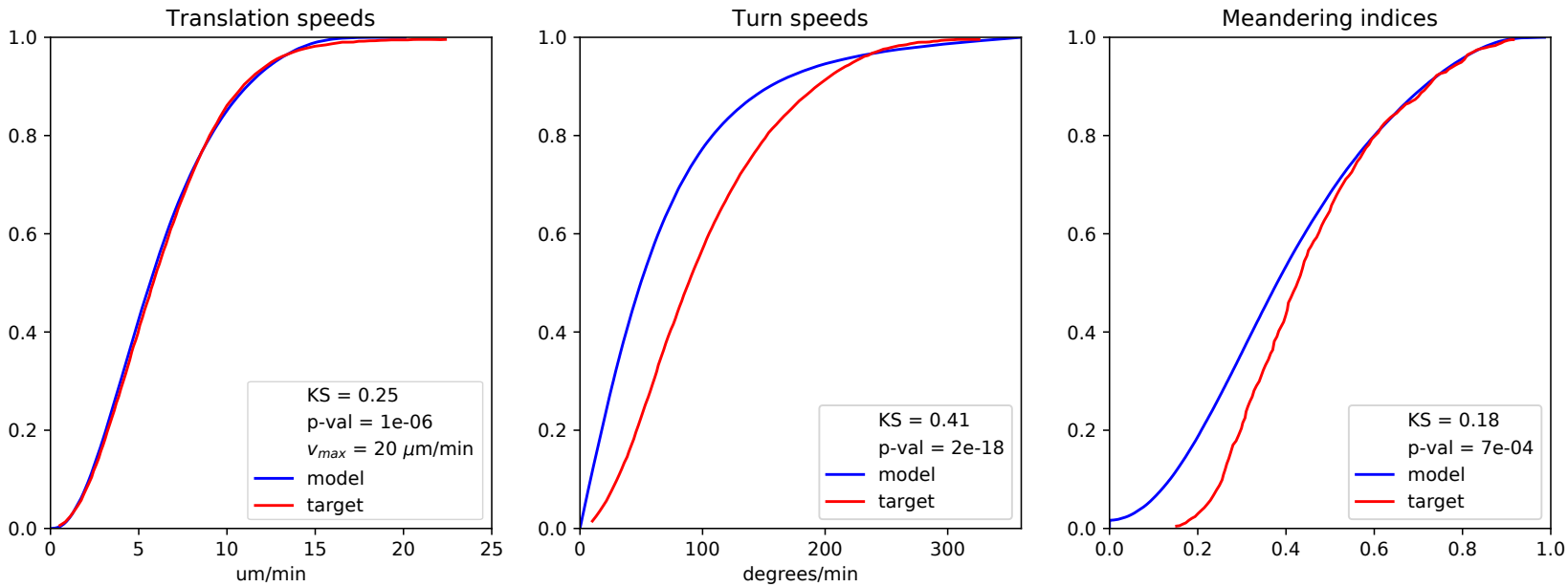

Figure 1: Red color denotes the CDFs obtained from simulations, blue color — target experimental CDFs[1].

[1]Read et al. Leukocyte Motility Models Assessed through Simulation and Multi-objective Optimization-Based Model Selection. 2016

Examples of simulated trajectories

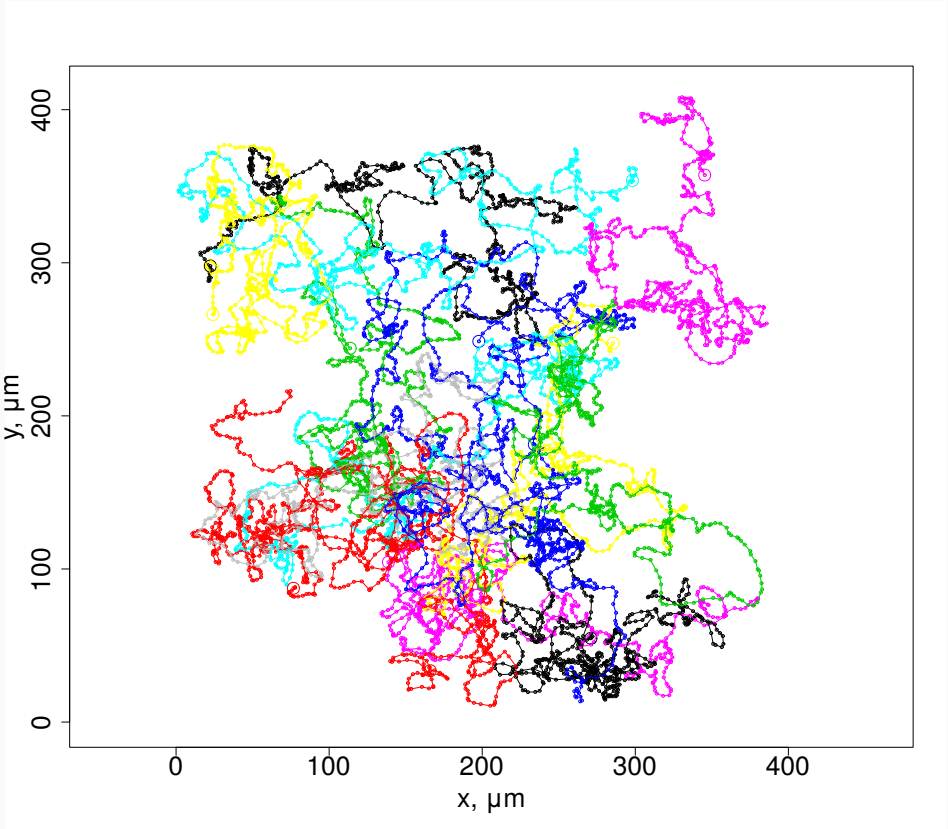

Figure 2: Examples of simulated trajectories of 15 randomly selected cells during 5 hours of simulation time.

The simulated fields of cell velocities and net forces

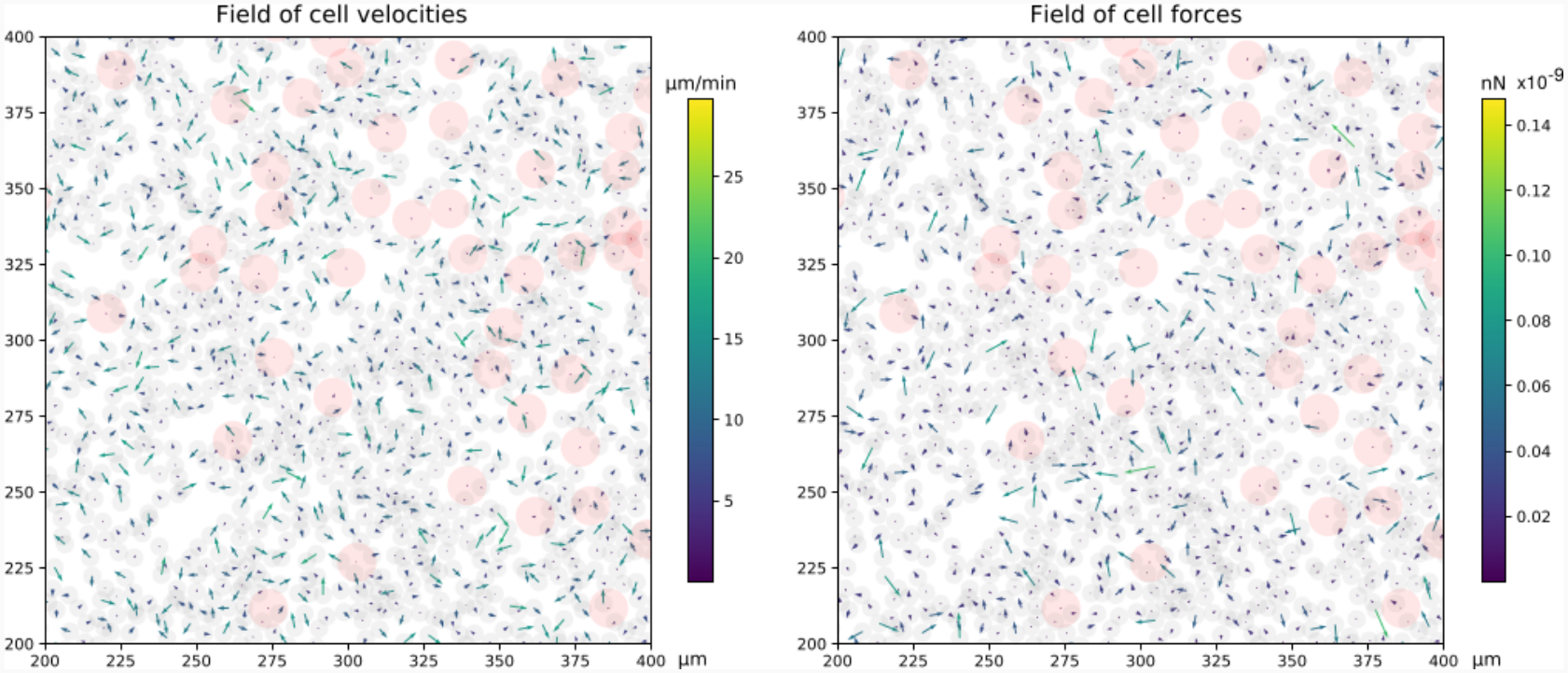

Figure 3: The field of (left) cell velocities and (right) net forces acting on the cells in a 100×100 μm^2 area of lymph node.

Model validation

Model validation
Immune response on Ovalbumin

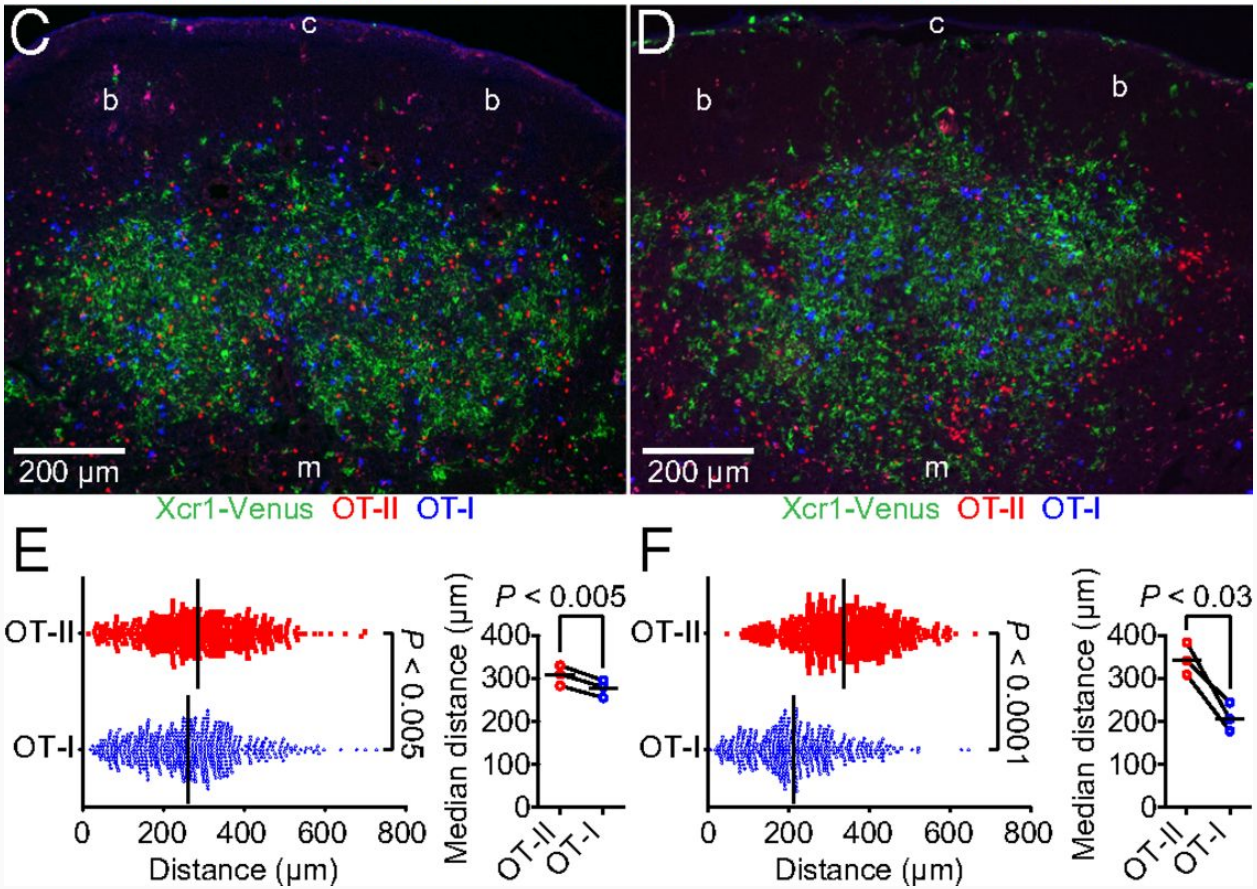

Kitano et al. Imaging of the cross-presenting dendritic cell subsets in the skin-draining lymph node. 2016

Model validation

Approximated lymph node geometry, configuration of initial state:

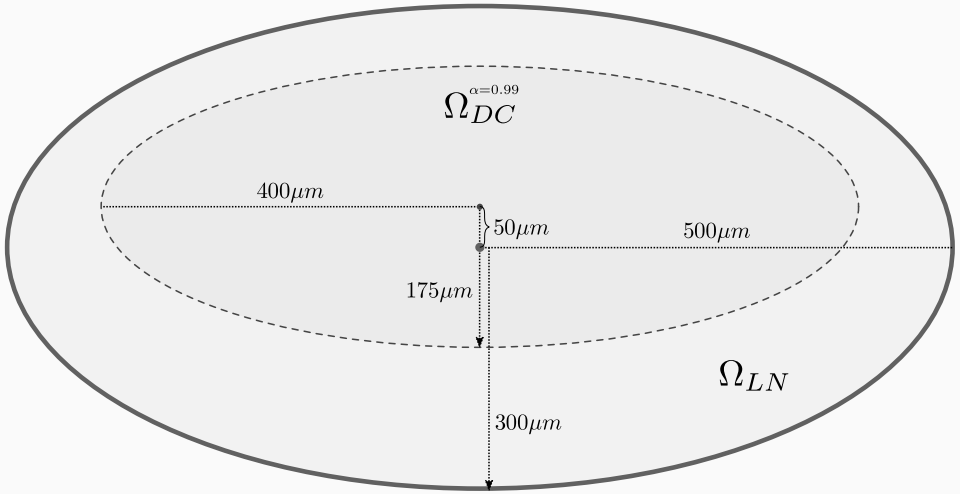

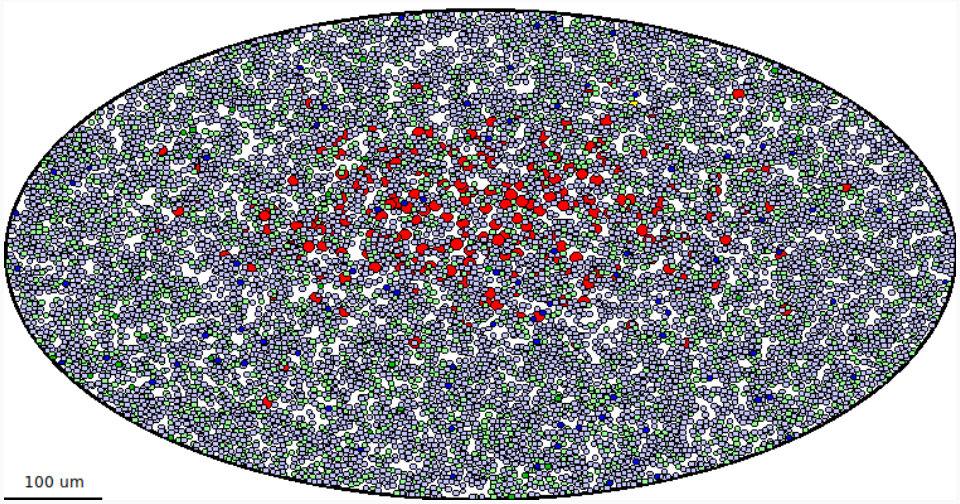

DCs: 234	Ag-specific CD4$^+$ TCs: 31	Ag-specific CD8$^+$ TCs: 86	Total: 12469
	Nonspecific CD4$^+$ TCs: 3272	Nonspecific CD8$^+$ TCs: 8846	

Spatio-temporal dynamics of immune response on Ovalbumin in lymph node

C

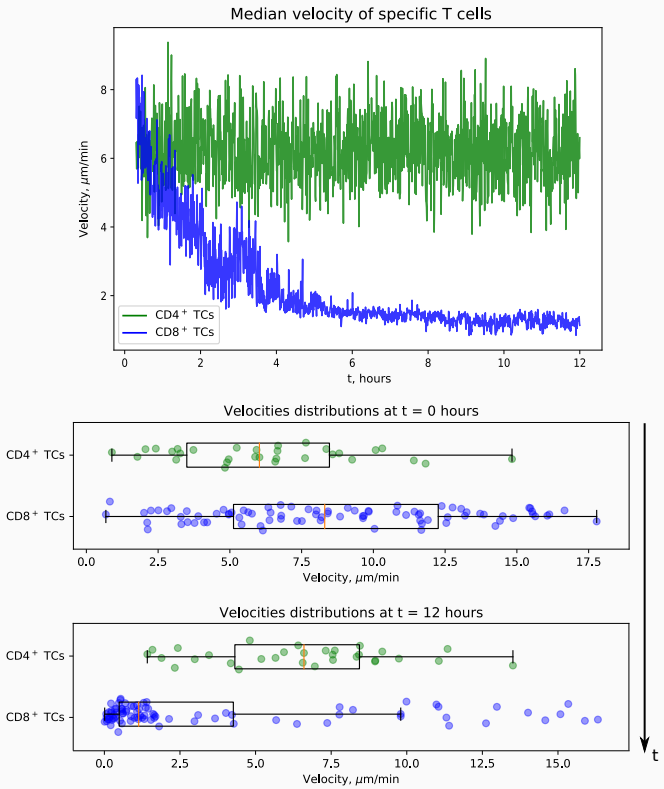

D

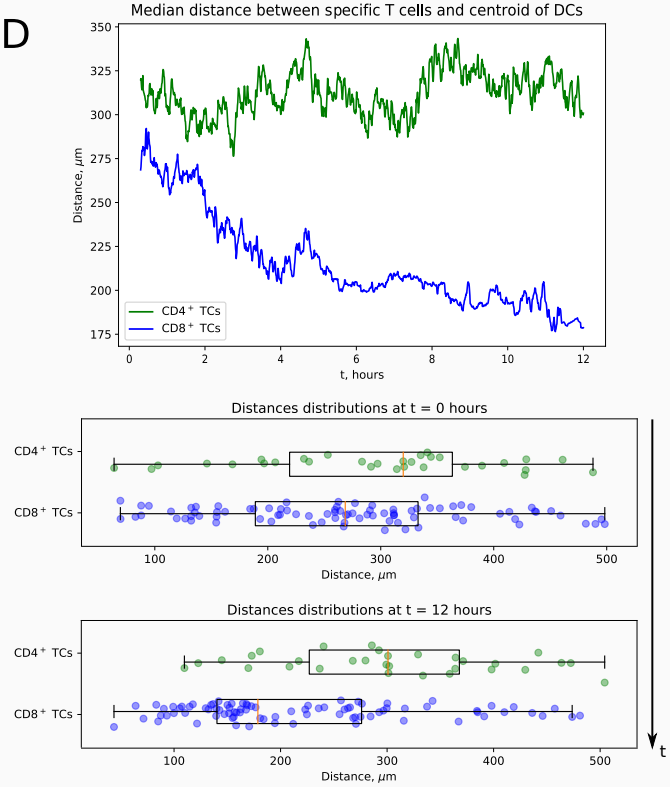

E

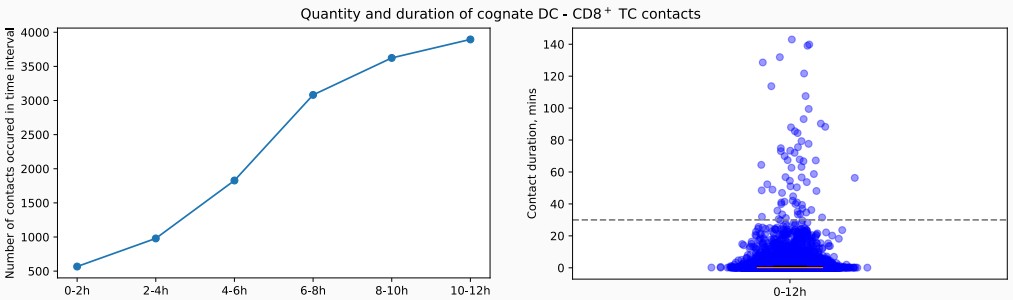

Model predictions

Conditions for timely detection of HIV-infected cells in LNs

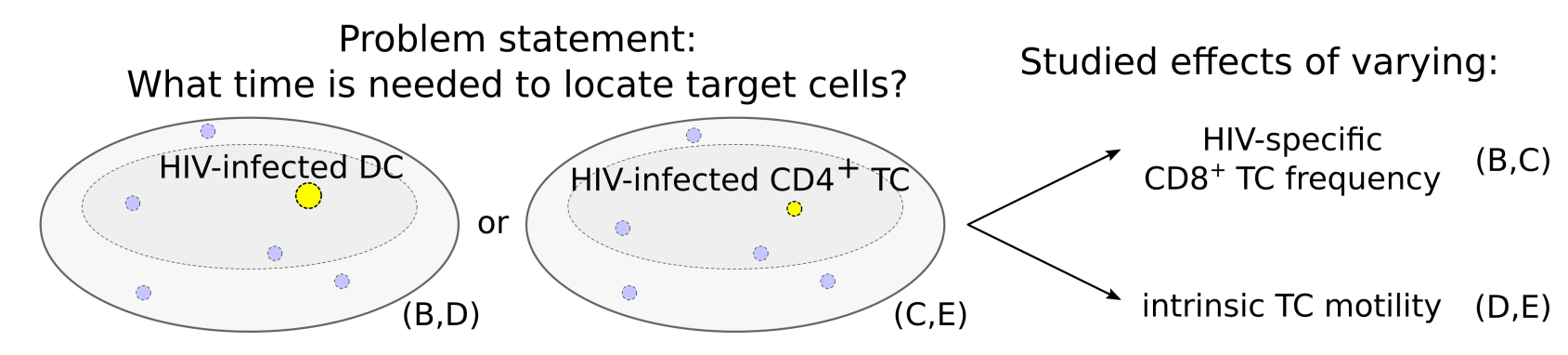

Conditions for timely detection of HIV-infected cells in LNs

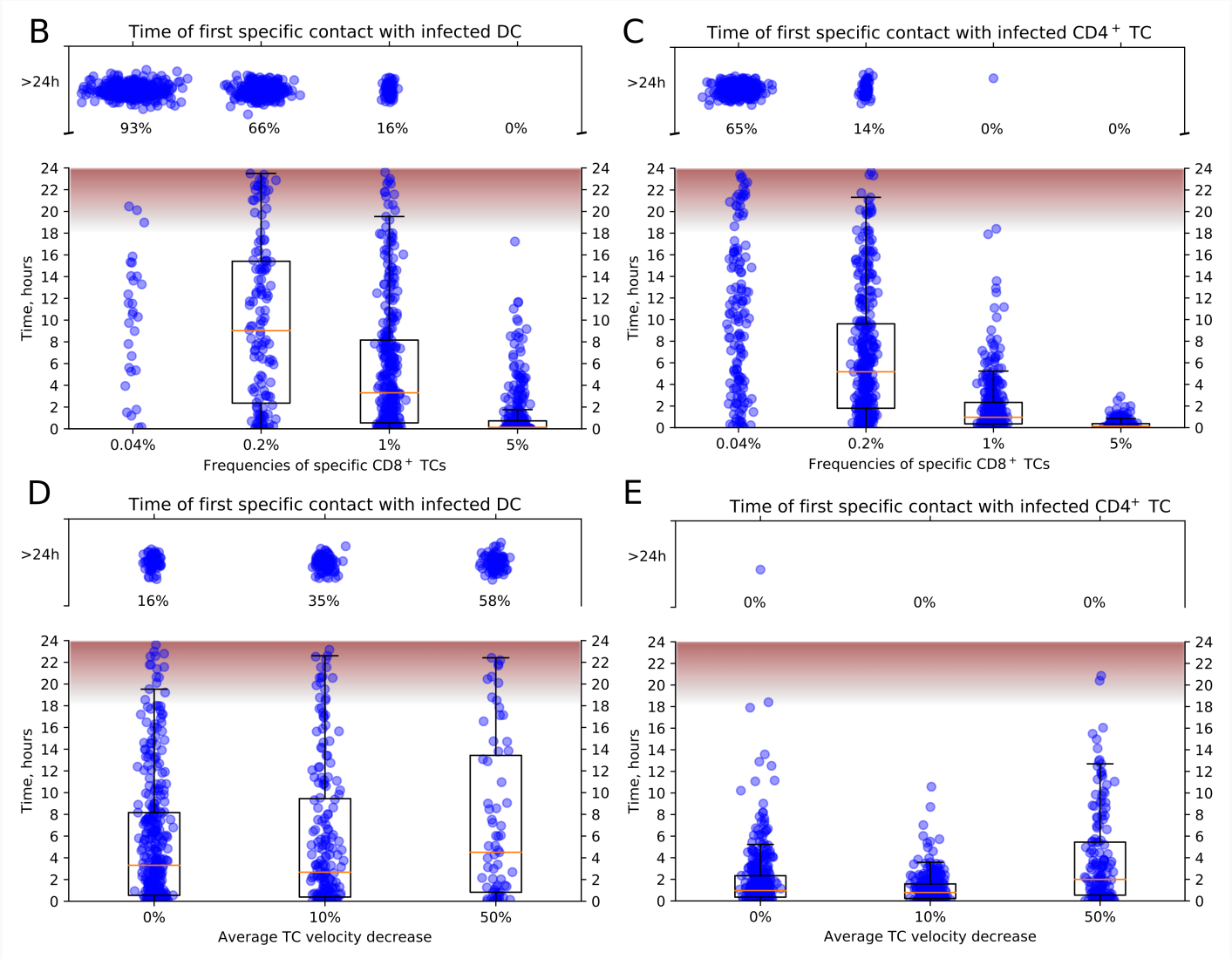

Grebennikov et al. Spatial Lymphocyte Dynamics in Lymph Nodes Predicts the Cytotoxic T Cell Frequency Needed for HIV Infection Control. 2019

Studying the HIV transmission in lymphoid tissue using multiscale model

Extracellular distributions of HIV virions and IFN molecules

- Free HIV virions $V(\mathbf{x}, t)$ are secreted by infected cells ($CD4^+$ T cells and DCs).
- Interferon molecules $I(\mathbf{x}, t)$ are secreted by productively infected DC.

Denoting $c = \{V, I\}$, we use reaction-diffusion equations with moving source terms:

$$\frac{\partial c}{\partial t} = D_c \Delta c + s_c - d_c c \quad \text{in} \quad \Omega_D,$$
$$c(\mathbf{x}, t) = 0 \ \text{ on } \ \partial\Omega_D, \ c(\mathbf{x}, 0) = 0 \ \text{ in } \ \Omega_D,$$

where s_c is a source term describing secretion of the virions or molecules by $N_c(t)$ corresponding cells: $s_c(\mathbf{x}, t) = \sum_{k=1}^{N_c(t)} \rho_c I_{\Omega_k}(\mathbf{x})$.

The reaction-diffusion equations are solved numerically using ADI method on a uniform rectangular grid.

Intracellular regulation of HIV transmission

Intracellular HIV replication cycle

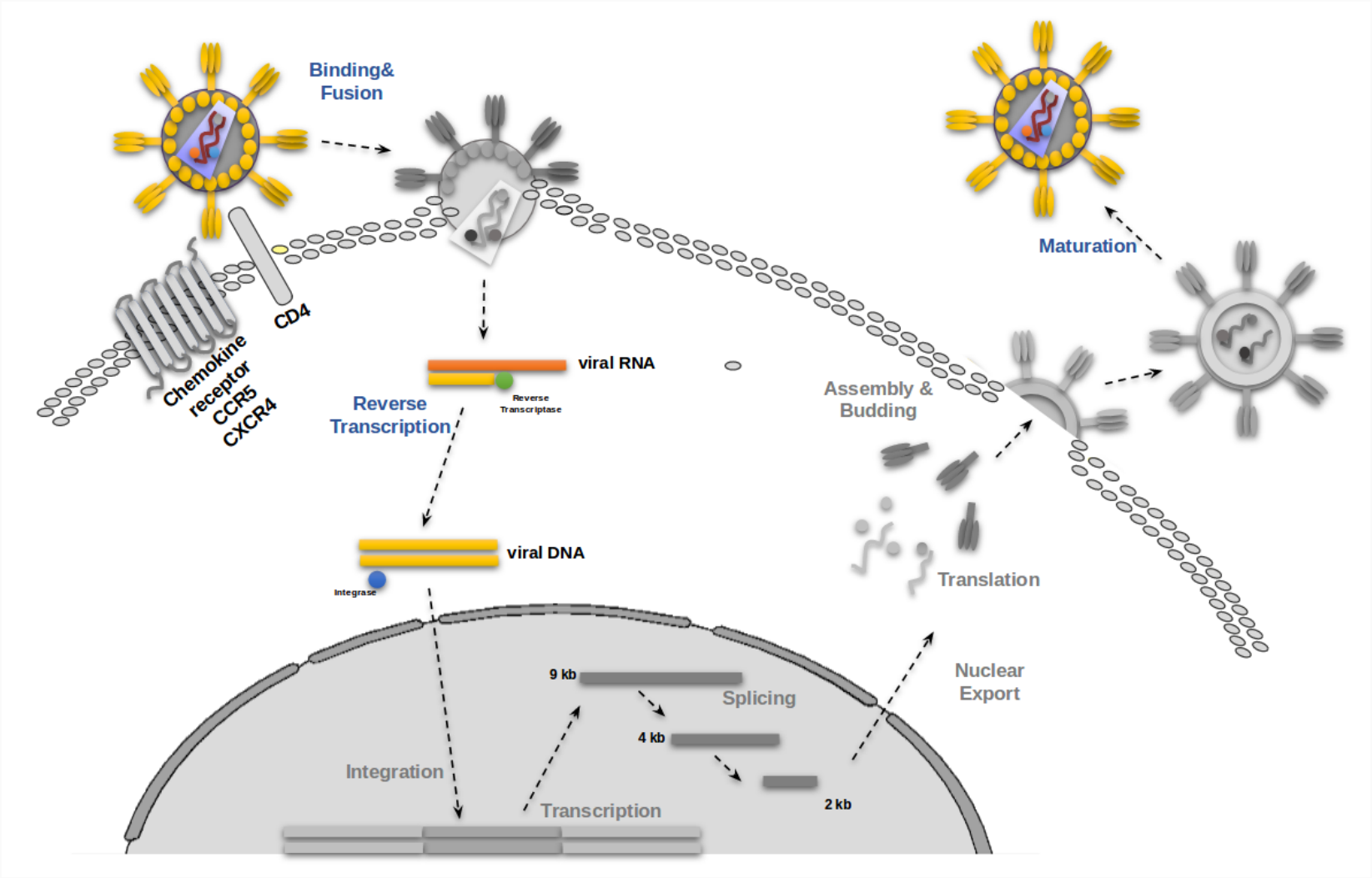

Intracellular HIV replication cycle

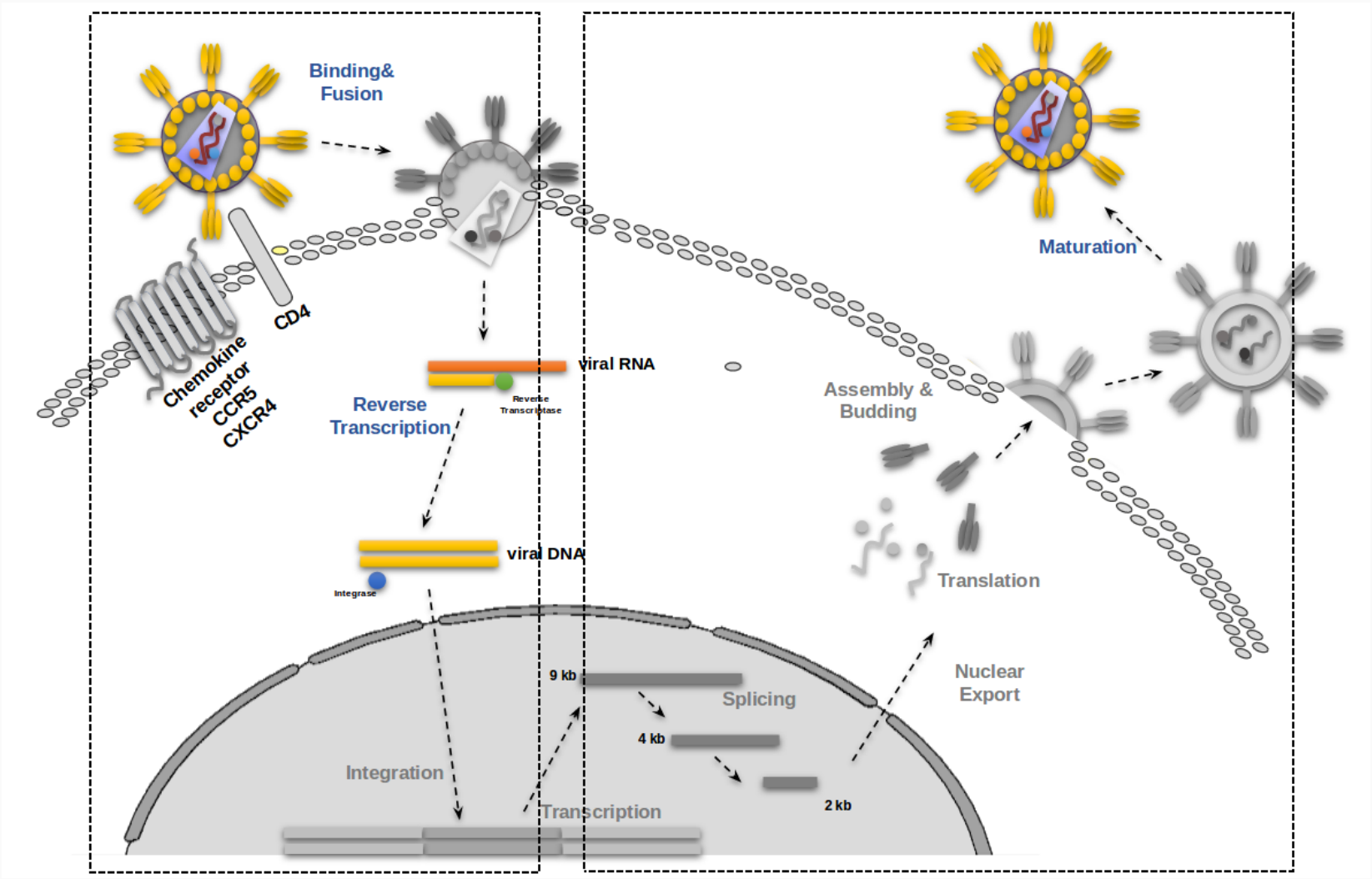

O. Orlova, Master Thesis, Moscow Institute of Physics and Technology, (2019).

Model of cell infection (integration of viral genome)

Cell infection by HIV involves two mechanisms:

- cell-to-cell transmission, $r^{(i)}_{cell} = \hat{k}^{(i)}_{cell}(t) \cdot N^{(i)}_{neigh}(t)$,
- infection by free virions, $r^{(i)}_{free} = \hat{k}^{(i)}_{free}(t) \int_{\Omega_i} V(\mathbf{x}, t) d\mathbf{x}$,

The CD4 molecules expression is being downregulated since the start of infection: $\hat{k}^{(i)}_{free}(t) = k_{free} \cdot e^{-(t-t^{(i)}_{inf})/t_d}$ and $\hat{k}^{(i)}_{cell}(t) = k_{cell} \cdot e^{-(t-t^{(i)}_{inf})/t_d}$.

The resulting stochastic model with time-dependent rates is simulated using Temporal Gillespie Algorithm. Main idea:

$$P(\tau|t^*) = \exp\left(-\int_{t^*}^{t^*+\tau} (k_{free} V_{\Omega_i}(t) + k_{cell} N^{(i)}_{neigh}(t)) e^{-(t-t^{(i)}_{inf})/t_d} dt\right),$$

$$P(\tau|t^*) = \exp\left(-\mathbb{L}(t^{**}|t^*)\right), \quad t^{**} = t^* + \tau,$$

1. Draw normalized waiting time $\tau' = \mathbb{L}(t^{**}|t^*) \sim \text{Exp}(1)$ from standard exponential distribution.
2. Time t^{**} when a next event will occur is given implicitly by the equation $\mathbb{L}(t^{**}|t^*) = \tau'$, which is solved numerically.

Model of cell infection (results of numerical simulations)

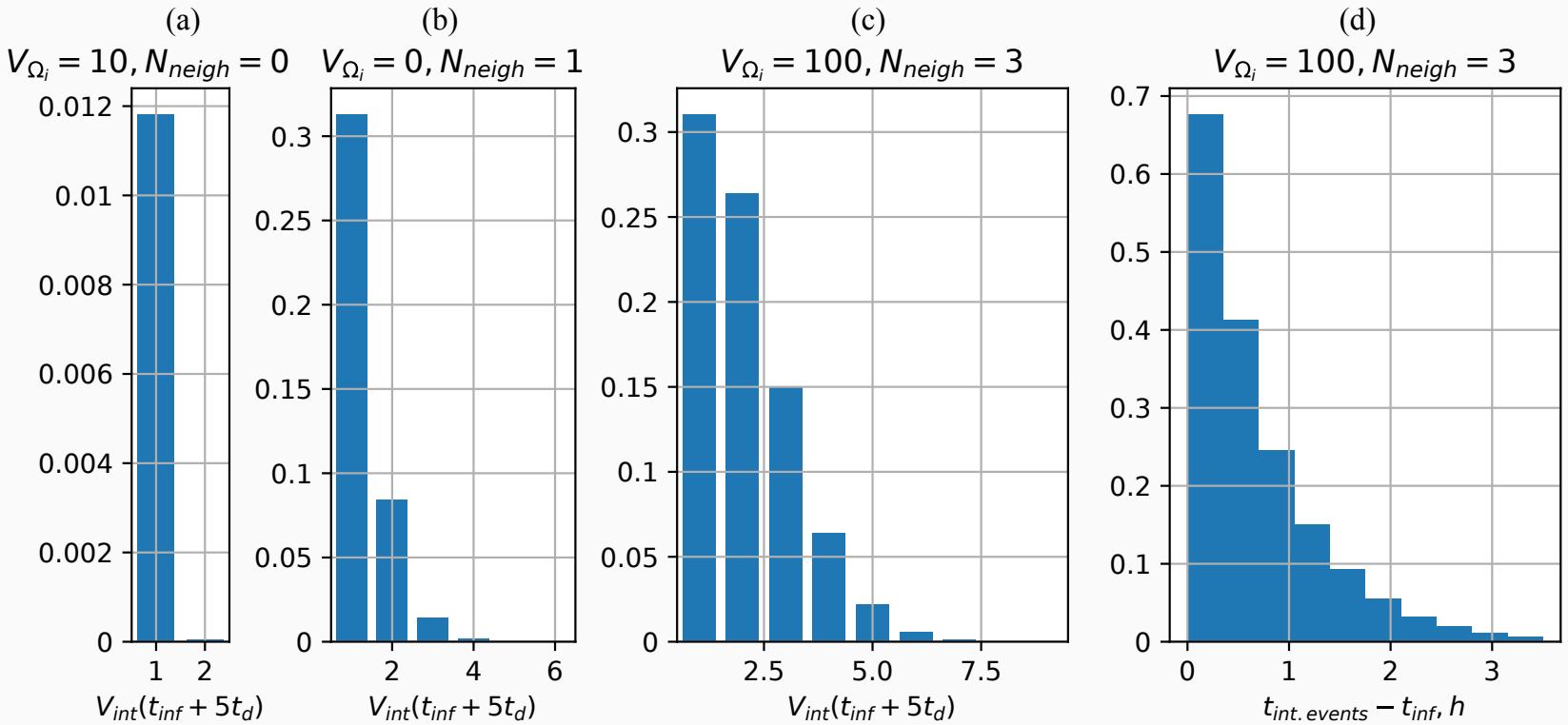

Figure 4: Distributions of integrated proviruses in the infected cell in different infection scenarios

Model of HIV replication

$$\frac{dV_{gRNAn}}{dt} = [TR] \cdot V_{int} - (2 \cdot k_{sp} \cdot (1 - \beta f_{Rev}) + k_{exp} \cdot f_{Rev} + d_{RNA}) V_{gRNAn},$$

$$\frac{dV_{dsRNAn}}{dt} = k_{sp} \cdot (1 - \beta f_{Rev}) V_{gRNAn} - (k_{exp} + d_{RNA}) V_{dsRNAn},$$

$$\frac{dV_{dsRNA}}{dt} = k_{exp} V_{dsRNAn} - (d_{RNA} + k_{ISG} \cdot b_{ISG}) V_{dsRNA},$$

$$\frac{d[Tat]}{dt} = r_{Tat} V_{dsRNA} - d_{Tat}[Tat], \quad \frac{d[Rev]}{dt} = r_{Rev} V_{dsRNA} - d_{Rev}[Rev],$$

$$\frac{dV_{gRNA}}{dt} = k_{exp} \cdot f_{Rev} \cdot V_{gRNAn} - (2 \cdot k_{mat} + d_{RNA} + k_{ISG} \cdot b_{ISG}) V_{gRNA},$$

$$\frac{dV_{mat}}{dt} = k_{mat} V_{gRNA} - (k_{\rho v} + d_{HIV}) V_{mat},$$

where $[TR] = [TR_{cell}] + f_{Tat} \cdot [TR_{Tat}]$,
$f_x = x/(1 + x + K_x V_{int}), x = \{Tat, Rev\}$.

The effect of b_{ISG} on V_{gRNA}, V_{dsRNA} will be described below.

Antiviral IFN response

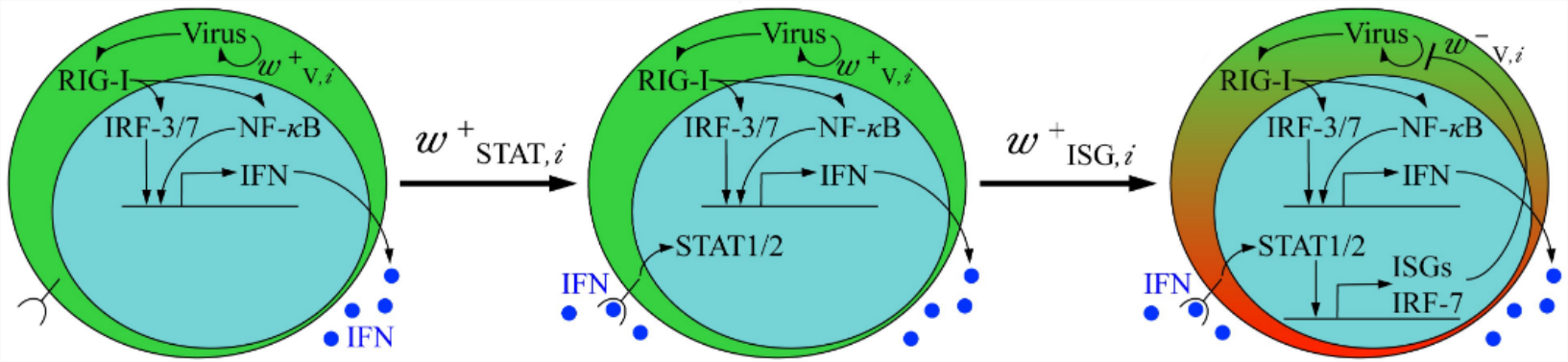

M. Rinas, Data-driven modeling of the dynamic competition between virus infection and the antiviral interferon response, PhD Thesis, University of Heidelberg, (2015).

Model of IFN response

Stochastic model of transitions between activation states:

- activation of STAT1/2 pathway (modelled as binary variable b_{ST}) by extracellular IFN-β I_{Ω_i}
- expression of interferon stimulated genes (ISGs) (modelled as binary variable b_{ISG}), which increase degradation rates of HIV RNA in cytoplasm V_{gRNA}, V_{dsRNA}

$$\{b_{ST} = b_{ISG} = 0\} \xrightarrow{a_{STAT}} \{b_{ST} = 1, b_{ISG} = 0\} \xrightarrow{r_{ISG}} \{b_{ST} = 1, b_{ISG} = 1\},$$

where
$a_{STAT}(t) = r_{STAT} \frac{I_{\Omega_i}(t)}{K_I + I_{\Omega_i}(t)}$ and r_{ISG} are propensity rates of transitions,
$I_{\Omega_i}(t) = \int_{\Omega_i} I(\mathbf{x}, t) d\mathbf{x}$.

The stochastic model with time-dependent rates is simulated using Temporal Gillespie Algorithm.

Intracellular dynamics of HIV and IFN in infected CD4$^+$ T cell

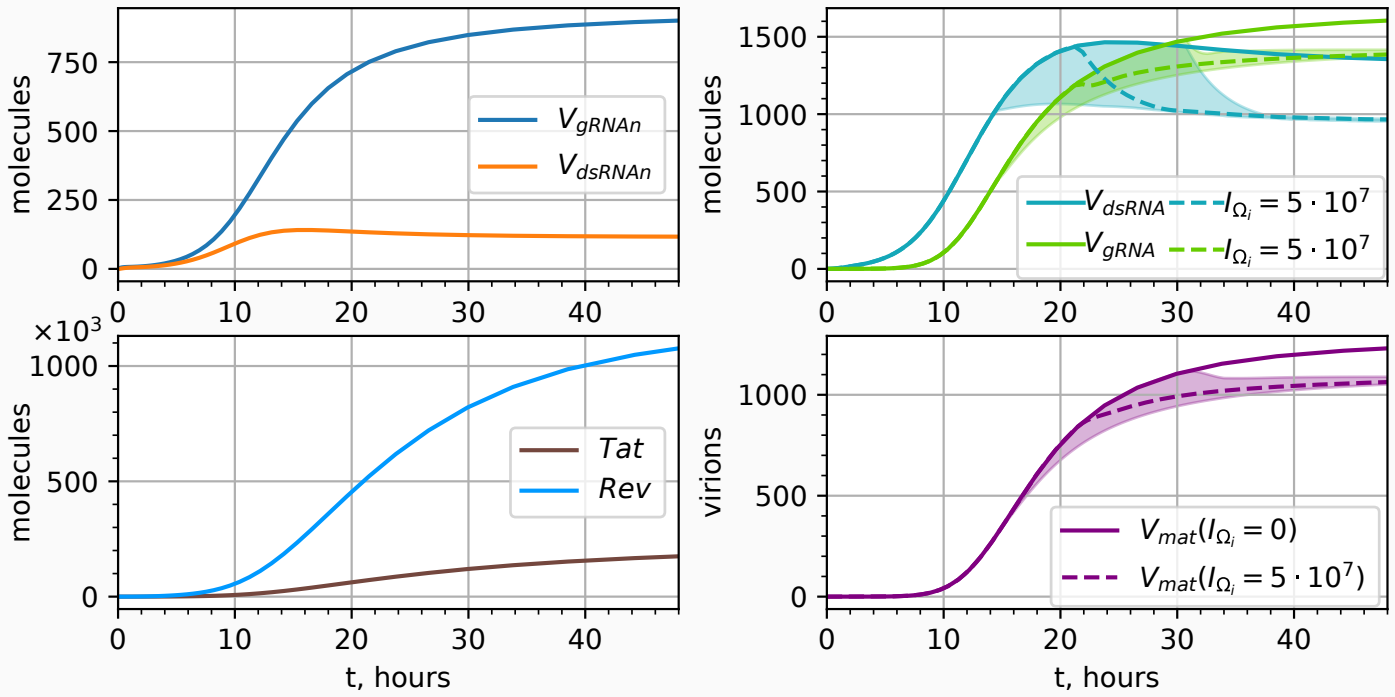

Figure 5: Intracellular HIV replication in productively infected cell with $V_{int} = 2$ integrated proviruses.

Numerical simulations of HIV infection dynamics in LN

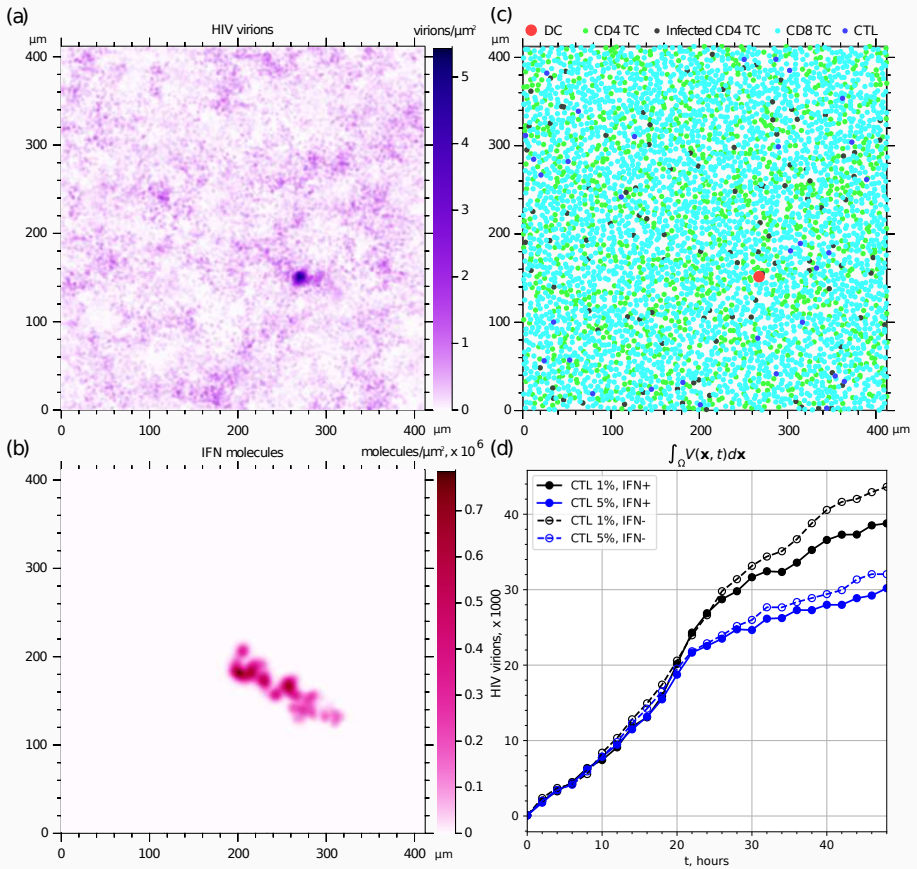

Figure 6: Extracellular fields of (a) HIV virions, (b) IFN molecules, and (c) the spatial distribution of cells (dendritic cell, infected and uninfected $CD4^+$ T cells, specific and nonspecific $CD8^+$ T cells) at 48 hours postinfection. (d) Temporal kinetics of total number of HIV virions in the computational domain during 48 hours postinfection at various immune conditions.

Results

- The spatial population dynamics of immune cells and humoral factors in lymphoid organs modelled with Newton's second law and reaction-diffusion equations, respectively calibrated using experimental data for 2D consideration.
- For intracellular processes of immune cell fate regulation, both deterministic and related stochastic models are developed in pairs, that describe HIV replication and antiviral IFN response.
- The model is used to predict the necessary conditions on CTL frequencies and motility which should be induced by HIV vaccine to block local bursts of HIV infection in lymph nodes, and the effect of antiviral IFN response on HIV transmission dynamics.

The work is supported by grant from Russian Science Foundation 18-11-00171

Further research for development of the multiscale model

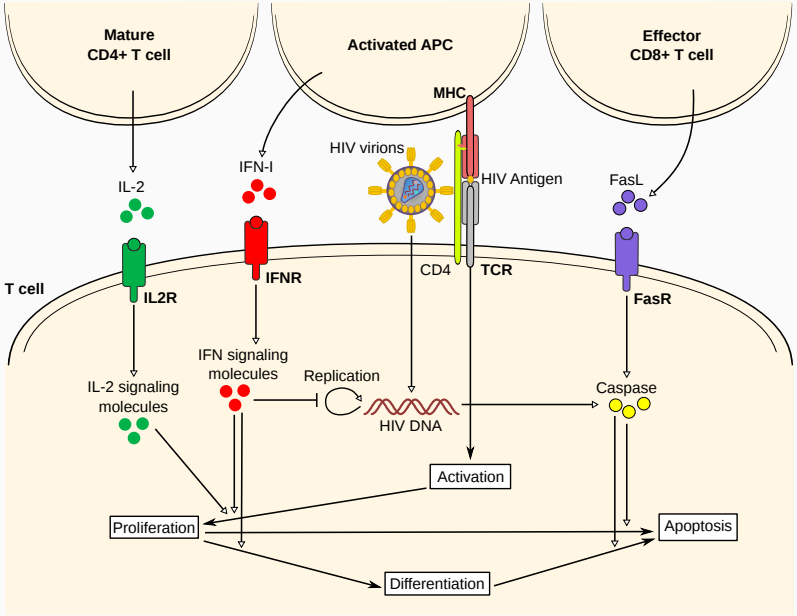

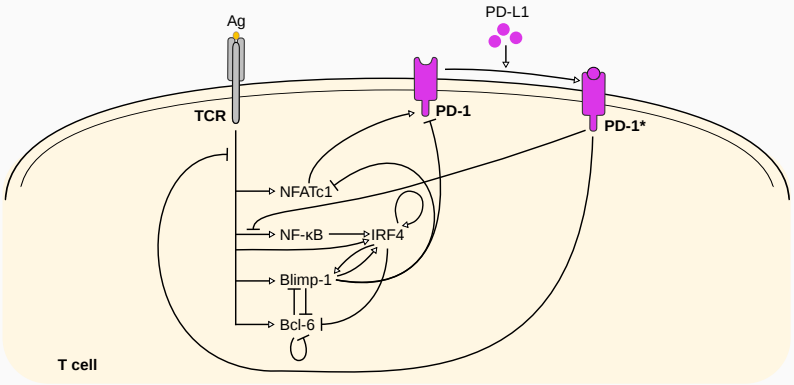

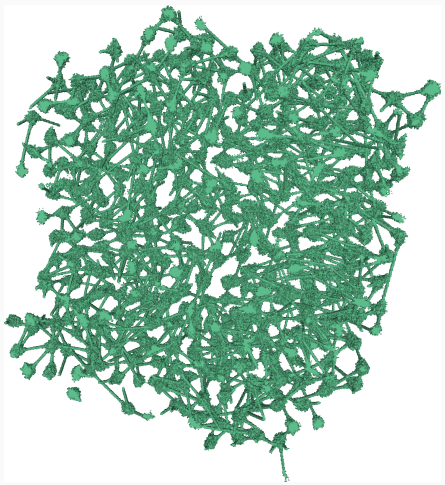

Grebennikov D.S. et al. Mathematical Modeling of the Intracellular Regulation of Immune Processes. Molecular Biology, 2019, 53(5), 815-829.,

Grebennikov D. et al. Critical Issues in Modelling Lymph Node Physiology. Computation, 2017, 5(1), 3.

Acknowledgements

- Bouchnita A (Uppsala University, Uppsala, Sweden)
- Volpert V. (Institut Camille Jordan, Lyon, France)
- Bessonov N. (Institute of Problems of Mechanical Engineering, Saint-Petersburg, Russia)
- Meyerhans A. (Universitat Pompeu Fabra, Barcelona, Spain)

Thank you for your attention!